Pharm Res (2015) 32:793–805
DOI 10.1007/s11095-013-1269-z

RESEARCH PAPER

Exploring the Wnt Pathway-Associated LncRNAs and Genes Involved in Pancreatic Carcinogenesis Driven by *Tp53* Mutation

Qi Wang • He Jiang • Chen Ping • Ruizhe Shen • Tingting Liu • Juanjuan Li • Yuting Qian • Yanping Tang • Shidan Cheng • Weiyan Yao • Lifu Wang

Received: 5 June 2013 / Accepted: 19 December 2013 / Published online: 28 January 2014

ABSTRACT

Purpose Study the contribution of long non-coding RNAs (lncRNAs) to progression of pancreatic intraepithelial neoplasia (PanIN) to pancreatic ductal adenocarcinoma (PDAC).

Methods We explored lncRNAs profilings in PanIN cell line (SH-PAN) isolated from *Pdx-1-Cre; LSL-Kras*$^{G12D/+}$ mice and PDAC cell line (DT-PCa) isolated from *Pdx-1-Cre; LSL- Kras*$^{G12D/+}$*; LSL-Tp53*$^{R172H/+}$ mice by lncRNAs microarray, and detected expression of lncRNAs and genes in PDAC by Real-time PCR, Western blot, ChIP and immunohistochemistry.

Results Eight lncRNAs and five protein-coding genes, associated with Wnt pathway, were identified with more than five-fold changes between DT-PCa cells and SH-PAN cells. Of them, lincRNA1611 and *Ppp3ca* were validated significantly high expression in DT-PCa cells and in 22 of 26 fresh resected human PDAC tissues, compared to SH-PAN cells and normal pancreatic tissues, respectively. Moreover, *Tp53* mutation status displayed a positive correlation with lincRNA1611 or *Ppp3ca* level. Immunohistochemical staining for Ppp3ca was weak or lack in 91 of 107 normal pancreatic tissues, 24 of 29 PanIN-I and 13 of 16 PanIN-II tissues, however, was strong in 10 of 27 PanIN-III and 62 of 107 PDAC tissues post operation.

Conclusions LincRNA1611 and *Ppp3ca* were high expression in PDAC and may serve as new potential targets for intervention of the disease.

Q. Wang, H. Jiang and C. Ping contributed equally to this work.

Electronic supplementary material The online version of this article (doi:10.1007/s11095-013-1269-z) contains supplementary material, which is available to authorized users.

Q. Wang • H. Jiang • C. Ping • R. Shen • T. Liu • J. Li • Y. Qian • Y. Tang • S. Cheng • W. Yao (✉) • L. Wang (✉)
Department of Gastroenterology, Ruijin Hospital, Shanghai Jiao Tong University School of Medicine, 197 Ruijin Er Road
Shanghai 200025, China
e-mail: yaowymail@sina.com
e-mail: lifuwang@sjtu.edu.cn

KEY WORDS *Kras* · lncRNA · pancreatic ductal adenocarcinoma · PanIN · *Tp53*

ABBREVIATIONS

ChIP	Chromatin immunoprecipitation
DT-PCa	PDAC cell line
lncRNAs	long non-coding RNAs
PanIN	pancreatic intraepithelial neoplasia
PDAC	pancreatic ductal adenocarcinoma
SH-PAN	PanIN cell line

INTRODUCTION

Pancreatic cancer, with an overall 5-year survival rate of <5%, is the fourth leading cause of cancer death in the past few years (1,2). The overwhelming majority of patients present with non-localized and metastatic diseases which is inoperable (3). *Tp53* is one of the most referenced and well-known pancreatic cancer suppressors which is inactivated in approximately 50%–75% of pancreatic cancers. Alterations of Tp53 protein function permit cells to bypass DNA damage checkpoints and apoptotic signals (4). Evidence is accumulating that loss of *Tp53* function may bring about genomic instability in pancreatic cancers (5,6). In addition, several studies have concluded that Wnt pathway play a crucial role in pancreatic carcinogensis (7–9). Can we hypothesize a connection between *Tp53* mutation and Wnt pathway-associated genes? In order to thoroughly confirm the hypothesis, lncRNA/mRNA expression profilings were identified. LncRNAs are understood as noncoding RNAs that longer than 200 and less than 100,000 nucleotides in length. LncRNAs take part in several intracellular regulation cascades, however, abnormal regulation of lncRNAs is determined to be mostly correlated to many diseases. There is a growing body of evidence pointing to the sense that lncRNAs exert key roles in several kinds of

carcinogensis (10–15). But little is known on the expression of lncRNAs and their biological functions in pancreatic cancer.

In our study, we applied the lncRNA/mRNA expression profiles in three pairs of PanIN cell line SH-PAN isolated from genetically engineered *Pdx-1-Cre; LSL-Kras$^{G12D/+}$* mutant mice and PDAC cell line DT-PCa isolated from the *Pdx-1-Cre; LSL-Kras$^{G12D/+}$; LSL-Tp53$^{R172H/+}$* compound mutant mice. The selected lncRNAs and protein-coding genes associated with Wnt pathway were further validated by real-time PCR and Western blot. Our results show that lncRNA/mRNA expression profiling may provide new molecular biomarkers for the pancreatic carcinogenesis.

MATERIALS AND METHODS

Patients and Tissue Samples

Fresh PDAC tissues from 26 patients and matched histological normal pancreatic tissues were obtained from patients who underwent surgery in the Department of Surgery at Ruijin Hospital in Shanghai. No patient received radiotherapy or chemotherapy before surgery. Tissues from each subject were snap-frozen in liquid nitrogen immediately after resection. Total RNA was extracted from 26 pairs of snap frozen PDAC tissues and matched histological normal pancreatic tissues using TRIzol reagent (Invitrogen, Carlsbad, CA, USA) according to the manufacturer's protocol.

Also, PDAC tissue samples and matched peritumoral tissue samples were obtained from 107 patients who underwent surgery in Ruijin Hospital in Shanghai. Tissue samples included peritumoral normal pancreatic tissues, PanIN tissues and invasive carcinoma. None of the patients had received radiotherapy or chemotherapy before surgery. After surgery, each tissue sample was fixed in formal and embedded in paraffin. Histological diagnosis was performed by two independent senior pathologists in the Department of Pathology in Ruijin Hospital.

Mouse Strain and Cell Lines

PanIN cell SH-PAN was isolated from the pancreas of a 4-month-old genetically engineered *Pdx1-Cre; LSL-Kras^{G12D}* mutant mice, and PDAC cell DT-PCa was isolated from the pancreas of *Pdx-1-Cre; LSL- Kras$^{G12D/+}$; LSL-Tp53$^{R172H/+}$* compound mutant mice as we previously described (5,6) (16). Both cell lines were grown in 10%FCS/DMEM/25 mM HEPES and supplemented with 100 U/ml penicillin, and 100 mg/ml streptomycin at 37°C with 5%CO_2.

Microarray and Computational Analysis

To extract total RNA, 1×10^6 SH-PAN and DT-PCa cells were harvested with the Trizol Reagent (Invitrogen, Carlsbad, CA, USA). Total RNA from each sample was quantified using the NanoDrop ND-1000 and the RNA integrity was assessed using standard denaturing agarose gel electrophoresis. For microarray analysis, Agilent Array platform was employed. The sample preparation and microarray hybridization were performed based on the manufacturer's standard protocols with minor modifications. Briefly, mRNA was purified from total RNA after removal of rRNA (mRNA-ONLY™ Eukaryotic mRNA Isolation Kit, Epicentre). Then, each sample was amplified and transcribed into fluorescent cRNA along the entire length of the transcripts without 3′ bias utilizing a random priming method. The labeled cRNAs were hybridized onto the Mouse LncRNA Array v2.0 (8×60 K, Arraystar). After having washed the slides, the arrays were scanned by the Agilent Scanner G2505B. Agilent Feature Extraction software (version 10.7.3.1) was used to analyze the acquired array images. Quantile normalization and subsequent data analysis were performed in the GeneSpring GX v11.5.1 software package (Agilent Technologies). After quantile normalization of the raw data, LncRNAs and mRNAs that at least 1 out of 6 samples have flags in Present or Marginal ("All Targets Value") were chosen for further data analysis. Finally, Hierarchical Clustering was performed to show the distinguishable LncRNAs and mRNAs expression pattern among samples.

Coexpression Network

Gene-coexpression networks were built according to the normalized signal intensity of differentially expressed genes. We constructed the network adjacency between two genes, defined as a power of the Pearson correlation between the corresponding gene-expression profiles. To make a visual representation, only the strongest correlations (0.99 or greater) were drawn in these renderings. In gene-coexpression networks, each gene corresponds to a node. Two genes are connected by an edge, indicating a strong correlation (i.e., either positive or negative).

Reverse Transcription and Quantitative Real-Time PCR Assay

To validate gene expression changes,Reverse transcription and quantitative real-time PCR were employed. The primer sequences are shown in Table I. The assays were done using ABI PRISMs 7300 Sequence Detection System (Applied Biosystems, Foster City, CA, USA). The relative quantification of lncRNAs and mRNAs expression was determined using the comparative C_T method. LncRNAs and mRNAs

Table I Primers Used in this Study

Name	Sequence (5′-3′)	Product size
ENSMUST00000052615	F CATTGTTCCTGGGTCGTGC R TTGGTGATCTCGGAGCTGG	191
ENSMUST00000122008	F AATGAACCGCCCTGCTCCT R AACATGAATGCCTTCTTTCTCCAC	187
ENSMUST00000110798	F AAGGCCAAGATTGAAGATGAGA R CCGCATCCTGTAAGTCTTTGTT	264
ENSMUST00000119417	F TGAGCAGTATGCCTGGGAGTC R AGTAATGGGATAGCCAATGAAGTG	183
ENSMUST00000170943	F TGGCACATCAGGTGTTCGTT R CATTGGCAGTATCAGGACTATTTG	215
ENSMUST00000120497	F TTTGTAGAGCCCAGTCAGCAGT R ATGAAGAAGCCAGTGAATCCTATG	143
ENSMUST00000056452	F AGAAGCCGATGTAGGACCGTAT R AATGGGTTGGAAGAAGCCACT	236
LincRNA1611	F CCATCTGCCTTACTCTTTCCTC R GTGTAGGGCACACTTGTTAAGG	111
HMlincRNA1611	F GCCATCTGCCTTACTCTTTCCT R GTGTAGGGCACACTTGTTAAGG	112
Rac1	F AGTTCCCTGTCACAGAGGTTGT R ATTACACAGGAGGCTGAAGAGC	187
Rhoa	F ACACTGCTCTAACAGCCCTCTC R CACCAGAGTTCTTGCAGTTGAC	180
Ruvbl1	F GTTTATGAAGGGGAGGTGACAG R TCCAGCCTCTACTCGTTCTTTC	177
Ppp3ca(murine)	F GTGTGTACACGGTGGTTTGTCT R GTACGAACAGCCTCTGACTGTG	187
Ppp3ca(human)	F GAGTACTTTCTGGAGGGAAGCA R AGTCTCTGAGGTGAGAGCCTTGT	218
Ppp3ca(ChIP)	F AGAGTCTCTCTAGCCCACAGGTC R CTGTCTCTTTGTCTCTGGCTCTC	249
Ppp3cb	F TTCTCAGGGAGGAGAGTGAAAG R GGTGGAGAGAATCCTCGTATTG	157
Ppp2r1a	F CCTGGCTAGTGGATCATGTCT R CTGCCATACGAAGAACTGTGG	243
Skp1a	F TTACTGAAGAGGAAGAGGCCC R GAAGAAACTCAGCCACAGGTC	220
Ppp2r5e	F CCTGTGGAGTAAGAGAGAGAGCA R GGTGAGCTAGAGAAGGAGGATGT	208
Ctbp2	F CCAACTCCAGTCAGGTCTACAAC R GTAGGCCCATAGCCTCTATTCAG	166
Wnt11	F TGTATCTACAGAGCTCCCCTGAC R CCAGTGGTACTTGCAGTGACAT	185
Wisp1	F CCACTAGAGGAAACGACTACACG R CACACACTCCTATTGCGTACCTC	235
Mapk9	F CTGAGACACCTGTCTATGGCTTC R CATAGCACACTCCCCTTACAGTG	189
Ctbp1	F CACTGACCAGAGAAGATCTGGAG R ATCTGCTCTACACTCTGGACTCG	247
Ppp2r5d	F GAGTGCTCAGTGCTTAGACAACC R GGAGAGGAGAGACACCTCAACTT	152
Plcb1	F CCAGACAGTGGATCTAGCTATGC R CCACTTCCACATAAGTCCCAAC	221
Cul1	F AGAGGAAGACCGCAAACTACTG R CTGTAGGTGTCCTTCTCACCATC	210
Ppp3r1	F GGTATTAGGCCAGCTCTTTTCC R CAGCACTGAACTAGACCTCCAAC	202
human GAPDH	F AGAAGGCTGGGGCTCATTTG R AGGGGCCATCCACAGTCTTC	258
murine GAPDH	F GGTGAAGGTCGGTGTGAACG R CTCGCTCCTGGAAGATGGTG	233

expression in DT-PCa cells relative to the SH-PAN cells was calculated using the following formulas: $\Delta\Delta CT = \Delta CT$ DT-PCa—ΔCT SH-PAN, fold change $= 2^{-\Delta\Delta CT}$ (17).

Western Blotting Analysis

Preparation of whole-cell lysates and electrophoresis were done as we described previously (18). All primary antibodies used were rabbit polyclonal anti-mouse antibodies, including Rac1 antibody (1:1,000, ab78139, Abcam, UK), Rhoa antibody (1:1,000, ab68826, Abcam, UK), Ppp3ca antibody (1:1,000, ab3673, Abcam, UK), Ruvbl1 antibody (1:1,000, ab51500, Abcam, UK), Ppp3cb antibody (1:1,000, ab96573, Abcam, UK). HRP-conjugated goat anti-rabbit IgG antibody (1:3,000, Imgenex) was used as secondary antibody. Immunodetection was carried out using the ECL Western-blotting detection kit (Amersham Corp, UK). Relative protein expression levels were quantified by densitometric measurement of ECL reaction bands and normalized with values of GAPDH.

Chromatin Immunoprecipitation

Chromatin immunoprecipitation (ChIP) was performed using the EZ ChIP™ Chromatin Immunoprecipitation Kit (Millipore Bedford, MA, USA) according to its manual. The chromatin was immunoprecipitated using Tp53 rabbit polyclonal anti-mouse antibody (Cell Signaling Technology). Normal rabbit polyclonal anti-mouse antibody IgG was used as negative control. Primer sequences are listed in Table I.

Histology and Immunohistochemistry

Detailed procedures are provided as we described previously (19,20). Briefly, tissues were fixed in 10% formalin overnight and then embedded in paraffin. Serial 5-μm thick sections from the tissue blocks were cut, and were dried overnight in a 60°C oven. The sections were dewaxed in xylene and dehydrated through graded alcohol to water, and then were stained in H&E for histological verification. For immunohistochemistry, the sections were dried overnight in a 60°C oven and then dewaxed in xylene, rehydrated through graded alcohol to water. After antigen retrieval with 0.01% EDTA (pH 8.0), endogenous peroxidase activity was blocked with 1% hydrogen peroxide in distilled water for 25 min followed by washing with distilled water and finally PBS + 0.1% Tween for 5 min. Rabbit anti-mouse polyclonal antibody to Ppp3ca (1:75, PAB10422, Abnova) was used as the primary antibody. Signal detection was accomplished with biotinylated anti-rabbit secondary antibody (1:200, Santa Cruz) using the Elite Vectastain ABC kit and peroxidase substrate DAB kit (Vector Laboratories, Burlingame, CA). The evaluation of immunohistochemical staining of Ppp3ca in PDAC and paired peritumoral tissues was defined as detectable immunoreaction in perinuclear and/or cytoplasm and was semi-quantitatively estimated from intensity of staining as previously described (19,20): grade 0 (no staining), grade 1 (weak staining), grade 2 (moderate staining) and grade 3 (strong staining). The percentage of positive cells was scored from grade 0 to grade 3. Grade 0, <1% of the cancer cells stained or with complete absence of staining; Grade 1, 1% to 49% positive expression; Grade 2, 50% to 70% positive expression; and Grade 3, >70% positive expression.

Statistical Analysis

All the statistical analyses were performed using SPSS version 17.0 software. The results were presented as means ± SD. Significant changes were assessed using Student's *t* tests, and *p* values < 0.05 was considered significant. To determine the correlation between *Tp53* mutation status and lincRNA1611 levels in the human pancreatic carcinoma specimens, Wilcoxon Rank–Sum test was used.

RESULTS

Overview of LncRNAs/mRNAs Profiles

In our study, Arraystar Mouse LncRNA Microarray v2.0 is designed for the global profiling of mouse lncRNAs and protein-coding transcripts. 15035 lncRNAs and 12442 coding transcripts can be detected by our second-generation lncRNA microarray. The lncRNAs are carefully collected from the most authoritative databases such as RefSeq, UCSC Known genes, Ensemble and many related literatures. Each transcript is represented by a specific exon or splice junction probe which can identify individual transcript accurately. Positive probes for housekeeping genes and negative probes are also printed onto the array for hybridization quality control. From the microarray data, we compared the lncRNAs/mRNAs expression levels and identified 319 upregulated lncRNAs, 571 downregulated lncRNAs (≥2-fold changes) in DT-PCa cells compared to SH-PAN cells (Table S1). A collcetion of most significantly up-regulated and down-regulated lncRNAs with more than five-fold changes was listed in Table II. From these differentially expressed lncRNAs, we listed 105 lincRNAs (large intergenic noncoding RNAs) with more than two-fold changes (Table III). The lincRNAs may locate on the upstream or downstream of the nearby coding genes (distance <300 kb). Up to 12,442 detected coding transcripts probes, we discovered 1,106 upregulated mRNAs, 407 downregulated mRNAs (≥2-fold changes) in PDAC cell DT-PCa compared with PanIN cell SH-PAN (Table S2). We next categorized the signaling pathways identified through microarray assay. Using Ingenuity Pathway Analysis, we determined the genes were involved in more than 20 different signaling pathways. The most prominent of these pathways was the Focal adhesion, Wnt, cell cycle, tight junction, Jak-STAT signaling pathways and so on (Table S3).

In order to identify differentially expressed lncRNAs or mRNAs with statistical significance, we performed a volcano plot filtering between the two compared groups respectively. The threshold was fold change ≥2.0, *p*-value < 0.05 (Fig. 1a and c). Hierarchical clustering is one of the most widely used clustering methods for analyzing RNA expression data. Cluster analysis arranged samples into groups based on their expression levels, which allowed us to hypothesize the relationships among samples. The dendrogram showed the relationships among lncRNA or mRNA expression patterns of samples (Fig. 1b and d).

Alteration of Wnt-Associated LncRNAs/mRNAs Expression

Based on the key role of Wnt pathway in carcinogenesis, we subsequently selected Wnt-associated lncRNAs/mRNAs through current data from the microarray and bioinformatics. According to the Pathway Analysis, we listed all 17 differentially expressed mRNAs in Wnt pathway (Table IV). In the

Table II A Collection of Differentially Expressed LncRNAs Detected by Microarray

Probe name	*p*-value	Fold-change	Regulation
ENSMUST00000117829	0.003829533	34.108944	Up
ENSMUST00000046048	0.002299617	33.67035	Up
ENSMUST00000118213	0.000993284	16.89885	Up
uc.186-	0.003658499	13.1048155	Up
AK014252	0.026357451	12.176874	Up
ENSMUST00000118595	0.020813918	11.079299	Up
uc.151-	0.000167235	9.999084	Up
ENSMUST00000170943	0.013751851	8.9420877	Up
ENSMUST00000165914	7.62415E-05	8.84859	Up
uc.273+	0.000583624	8.8479595	Up
ENSMUST00000112739	0.008886281	8.822593	Up
AK136617	0.022630807	8.756134	Up
ENSMUST00000120017	0.003264625	8.420138	Up
uc007zya.1	0.004015589	8.389156	Up
uc007zya.1	0.004015589	8.389156	Up
MM9LINCRN AEXON10767+	0.03282429	7.9865766	Up
uc.184+	0.001772575	7.9605846	Up
ENSMUST00000119775	0.004583005	7.8915124	Up
ENSMUST00000119417	0.022172816	7.666819	Up
NR_002688	0.003723377	7.5421114	Up
uc.209-	0.000141469	7.2929296	Up
ENSMUST00000121177	0.013207162	7.0755153	Up
uc009job.1	0.004733458	6.910349	Up
uc.49-	0.00180083	6.89423	Up
ENSMUST00000091539	0.011179222	6.7374606	Up
ENSMUST00000099421	0.004859604	6.715215	Up
ENSMUST00000117979	0.007174608	6.7051196	Up
ENSMUST00000163890	0.005269885	6.6237063	Up
ENSMUST00000091531	0.008961571	6.561031	Up
ENSMUST00000119947	0.000471556	6.533056	Up
ENSMUST00000094493	0.005256705	6.361041	Up
ENSMUST00000059005	0.002783112	6.248133	Up
uc007kkj.1	0.001143158	6.1706376	Up
ENSMUST00000122008	0.003659073	6.1474567	Up
ENSMUST00000056452	0.021287543	6.1374243	Up
ENSMUST00000119238	0.002083869	6.137277	Up
ENSMUST00000117261	0.001217181	6.0500607	Up
ENSMUST00000117618	0.00168203	6.0399666	Up
uc.174+	0.001439202	5.9911695	Up
ENSMUST00000118496	0.001952755	5.9305973	Up
ENSMUST00000166210	0.005769488	5.924425	Up
ENSMUST00000117655	0.005054969	5.8636107	Up
ENSMUST00000052615	0.006665169	5.7424192	Up
ENSMUST00000121523	0.03563393	5.7416496	Up
ENSMUST00000110798	0.005114431	5.650384	Up
NR_027854	0.00316021	5.5012436	Up
uc.36+	0.000282953	5.448959	Up
ENSMUST00000117327	0.003677156	5.446094	Up
uc007wbs.1	0.005994671	5.3940415	Up
ENSMUST00000100173	0.011249878	5.3913264	Up
ENSMUST00000118212	0.000913254	5.3312955	Up
ENSMUST00000167639	0.01022392	5.2465787	Up
uc007keu.1	0.000133751	5.237649	Up
uc009kyh.1	0.002227321	5.2110586	Up
ENSMUST00000121455	0.007004182	5.1586766	Up
uc.208-	0.036322936	5.149641	Up
CB272499	0.020108119	5.1269145	Up
AK142426	6.96229E-05	190.59375	Down
uc009kos.1	0.00983906	9.314714	Down
AK029924	0.005427233	9.277254	Down
ENSMUST00000120774	4.77211E-05	8.265101	Down
MM9LINCRN AEXON11305+	0.002507961	7.686753	Down
MM9LINCRNAEXON11592-	0.02255855	7.586677	Down
NR_003645	0.00463993	7.214379	Down
MM9LINCRN AEXON11053+	0.004277992	7.1100726	Down
ENSMUST00000170798	0.01752346	7.012389	Down
DV653238	0.002521146	6.9401426	Down
ENSMUST00000121026	0.00033688	6.384608	Down
ENSMUST00000120497	0.01856478	6.162123	Down
uc007nuv.1	0.018167166	6.1224294	Down
uc007qgm.1	0.040883314	5.896056	Down
AK080727	0.003327161	5.688554	Down
MM9LINCRNAEXON10060-	0.043102995	5.612416	Down
uc007ohk.1	0.000678434	5.5138907	Down
mouselincRNA1065-	0.018586649	5.504788	Down
ENSMUST00000120283	0.033822265	5.4676037	Down
CJ052491	0.003181188	5.296954	Down
ENSMUST00000130262	0.020005831	5.145877	Down
uc007qzv.1	0.010667391	5.112347	Down
ENSMUST00000153669	0.003216897	5.0930614	Down

lncRNAs with more than five-fold changes are listed here

coexpression network, five protein coding genes in Wnt pathway displayed a strong correlation with eight lncRNAs (Fig. 2a) (Table S4). Next, the eight lncRNAs (lincRNA1611, ENSMUST00000052615, ENSMUST00000122008, ENSMUST00000110798, ENSMUST00000119417, ENSMUST 00000 170943, ENSMUST00000120497, ENSMUST00000056452) and the five mRNAs (*Rhoa*, *Rwbl1*, *Rac1*, *Ppp3ca*, *Ppp3cb*) were selected to validate the consistency by real-time PCR. Results showed a strong consistency in all the selected lncRNAs and mRNAs between the real-time PCR results and microarray data (Fig. 2b). Of them, seven lncRNAs and five protein coding genes were upregulated in DT-PCa cells,

Table III lincRNAs and Nearby Protein-code Genes

Seqname	*p*-value	Fold change	Regulation	Gene symbol	Relationship
MM9LINCRNAEXON10784-	0.00157	2.8910859	Down	Man1c1	Downstream
CB317809	0.01036	3.0094671	Down	Las1l	Downstream
MM9LINCRNAEXON11623-	0.01148	2.417984	Up	Nln	Upstream
MM9LINCRNAEXON11624+	0.0009	3.1973174	Down	Nln	Downstream
MM9LINCRNAEXON11579-	0.01709	2.5690317	Down	Sfxn1	Downstream
ENSMUST00000142151	0.00019	2.3761501	Down	Tmem17	Upstream
MM9LINCRNAEXON10894+	0.0099	2.5548906	Down	Ahcyl1	Upstream
MM9LINCRNAEXON10894-	0.00785	2.7460945	Down	Ahcyl1	Downstream
ENSMUST00000117092	0.00627	2.496754	Up	Pls3	Downstream
MM9LINCRNAEXON11852+	0.04744	2.2290447	Down	Mfsd11	Upstream
uc007ixb.1	0.02968	2.0540106	Up	Il5	Downstream
MM9LINCRNAEXON11775-	0.0018	3.8249395	Down	Il5	Downstream
MM9LINCRNAEXON10152+	0.0459	4.308693	Down	Spsb4	Upstream
MM9LINCRNAEXON10767+	0.03282	7.9865766	Up	Gja4	Downstream
ENSMUST00000124191	0.01183	2.5711803	Down	Zfand6	Downstream
BQ552649	0.0112	2.5442438	Down	Irf2bp2	Upstream
ENSMUST00000121490	0.00592	3.0820146	Up	Cav3	Upstream
MM9LINCRNAEXON11715+	0.00231	2.8172164	Down	Gstz1	Downstream
AK141055	0.00074	3.4974248	Down	Trmt5	Upstream
ENSMUST00000166559	0.03299	2.7404857	Down	Ddx59	Downstream
MM9LINCRNAEXON12078-	0.04271	3.2521114	Down	Ddx59	Downstream
MM9LINCRNAEXON10430-	0.04328	3.52606	Down	Hoxa10	Upstream
MM9LINCRNAEXON11352+	0.0183	2.6202123	Down	Mgat3	Downstream
MM9LINCRNAEXON11353-	0.00077	3.64261	Down	Mgat3	Upstream
CB317809	0.01036	3.0094671	Down	Msn	Upstream
MM9LINCRNAEXON11427-	0.00606	3.7073677	Down	Dupd1	Upstream
AK188366	0.00982	2.3156607	Up	Rnf215	Downstream
BU843812	0.02317	2.2553768	Down	Eif2c2	Downstream
MM9LINCRNAEXON10784-	0.00157	2.8910859	Down	Sepn1	Downstream
MM9LINCRNAEXON10416-	0.02587	3.870585	Down	Mkln1	Upstream
ENSMUST00000142151	0.00019	2.3761501	Down	Commd1	Downstream
AK087822	0.00099	4.0685444	Down	Nek4	Downstream
AW120561	0.04805	2.187432	Down	Pabpc1	Upstream
MM9LINCRNAEXON10810+	0.00093	2.4643328	Down	Nceh1	Downstream
MM9LINCRNAEXON10060-	0.0431	5.612416	Down	Gm7157	Upstream
AK013346	0.01374	3.447062	Up	Gm7157	Upstream
MM9LINCRNAEXON11815+	0.00354	2.1277382	Down	Ube2z	Upstream
AV223046	0.00422	3.523497	Down	Styxl1	Upstream
AV223046	0.00422	3.523497	Down	Rasa4	Downstream
MM9LINCRNAEXON10981-	0.01104	2.6944637	Down	Hnrnpa3	Upstream
MM9LINCRNAEXON10894-	0.00785	2.7460945	Down	Gnai3	Upstream
MM9LINCRNAEXON10894+	0.0099	2.5548906	Down	Gnai3	Downstream
BB670232	0.02904	2.6186574	Down	Ctss	Upstream
MM9LINCRNAEXON11926-	0.00192	2.659616	Down	Appl2	Downstream
MM9LINCRNAEXON11025-	0.00367	2.6219437	Down	Bcl2l11	Downstream
ENSMUST00000154173	0.02	2.531439	Down	Bcl2l11	Downstream
ENSMUST00000154066	0.0491	2.5040698	Down	Gmcl1	Upstream
lincRNA0926+	0.03199	3.789165	Down	Celf4	Upstream
lincRNA1611	0.02719	2.634767	Up	Ppp3ca	Upstream

Table III (continued)

Seqname	*p*-value	Fold change	Regulation	Gene symbol	Relationship
MM9LINCRNAEXON11828-	0.00163	3.4365048	Down	Srcin1	Downstream
MM9LINCRNAEXON10368-	0.03302	3.5500255	Down	Eif4g2	Downstream
MM9LINCRNAEXON11003-	0.02494	2.0891693	Down	Hsd17b12	Downstream
MM9LINCRNAEXON11775-	0.0018	3.8249395	Down	Slc22a21	Upstream
uc007ixb.1	0.02968	2.0540106	Up	Slc22a21	Upstream
BU843812	0.02317	2.2553768	Down	Ptk2	Downstream
lincRNA0813+	0.00843	4.3062725	Down	Morf4l1	Downstream
uc009deo.1	0.00706	2.03524	Up	Cpne9	Upstream
MM9LINCRNAEXON10767+	0.03282	7.9865766	Up	Zmym4	Upstream
MM9LINCRNAEXON10430-	0.04328	3.52606	Down	Hoxa2	Upstream
MM9LINCRNAEXON11003-	0.02494	2.0891693	Down	Ttc17	Upstream
MM9LINCRNAEXON10105-	0.01752	2.2569652	Down	Usp2	Upstream
MM9LINCRNAEXON10819-	0.00406	2.5359251	Down	Bbs7	Upstream
ENSMUST00000154066	0.0491	2.5040698	Down	Pcyox1	Downstream
CK619885	0.04383	2.3884876	Down	Exoc3	Upstream
uc007ixb.1	0.02968	2.0540106	Up	Sept8	Downstream
MM9LINCRNAEXON11775-	0.0018	3.8249395	Down	Sept8	Downstream
AW120561	0.04805	2.187432	Down	Ywhaz	Upstream
lincRNA2242+	0.00615	3.5699105	Down	Ywhaz	Upstream
BU938249	0.03503	2.638071	Down	Dnahc1	Downstream
AK145738	0.00116	3.1407607	Down	Necap1	Upstream
ENSMUST00000165226	0.03597	3.7811058	Down	Smc3	Downstream
MM9LINCRNAEXON10981-	0.01104	2.6944637	Down	Agps	Upstream
MM9LINCRNAEXON11030+	0.00467	2.9342089	Down	Dstn	Upstream
ENSMUST00000166210	0.00577	5.924425	Up	Ncbp1	Downstream
AK149715	0.00771	2.0741777	Down	Ptdss1	Downstream
mouselincRNA1106+	0.03867	2.2484114	Down	Bnc2	Downstream
AK016867	0.01028	2.906847	Down	St3gal4	Upstream
mouselincRNA0047+	0.00141	2.4652195	Down	Abcb6	Downstream
MM9LINCRNAEXON10410-	0.03714	2.574271	Down	Copg2	Downstream
MM9LINCRNAEXON10416-	0.02587	3.870585	Down	Copg2	Downstream
AK165039	0.00327	3.4398072	Down	Bre	Downstream
MM9LINCRNAEXON10544-	0.02989	4.7156405	Down	Bre	Upstream
MM9LINCRNAEXON11003-	0.02494	2.0891693	Down	Api5	Upstream
ENSMUST00000139659	0.00888	2.2970195	Down	Clec2g	Downstream
AK188366	0.00982	2.3156607	Up	Ccdc157	Downstream
AK037562	0.04807	2.3069668	Down	Asf1b	Downstream
MM9LINCRNAEXON10368-	0.03302	3.5500255	Down	Eif4g2	Downstream
MM9LINCRNAEXON10105-	0.01752	2.2569652	Down	Pvrl1	Downstream
lincRNA0813+	0.00843	4.3062725	Down	Morf4l1	Downstream
AK013908	0.01997	4.194358	Down	Ercc8	Upstream
BB617615	0.03778	2.4218428	Down	Ppm1a	Downstream
AK016867	0.01028	2.906847	Down	Srpr	Upstream
ENSMUST00000129191	0.01087	2.6670344	Down	Fyn	Downstream
BB670232	0.02904	2.6186574	Down	Adamtsl4	Upstream
CB272499	0.02011	5.1269145	Up	Rcbtb2	Overlap
ENSMUST00000121490	0.00592	3.0820146	Up	Lmcd1	Upstream
AK016867	0.01028	2.906847	Down	Pus3	Downstream
MM9LINCRNAEXON11320-	0.03582	2.2466812	Down	Il10rb	Upstream

Table III (continued)

Seqname	*p*-value	Fold change	Regulation	Gene symbol	Relationship
BQ552649	0.0112	2.5442438	Down	Pard3	Downstream
lincRNA0997+	0.03605	2.150435	Down	Rps7	Upstream
ENSMUST00000165226	0.03597	3.7811058	Down	Smndc1	Upstream
mouselincRNA1065-	0.01859	5.504788	Down	Hs2st1	Upstream
MM9LINCRNAEXON11797-	0.02779	2.6154323	Down	Cd68	Upstream
ENSMUST00000165226	0.03597	3.7811058	Down	Add3	Upstream
MM9LINCRNAEXON11592-	0.02256	7.586677	Down	Fam172a	Downstream

lincRNAs and nearby protein-code genes with more than two-fold changes are listed here

but only lncRNA ENSMUST00000120497 was downregulated in DT-PCa cells, compared to SH-PAN cells. Moreover, Western blot were also performed to test the protein level of Rhoa, Ruvbl1, Rac1, Ppp3ca, Ppp3cb. Results showed that protein levels of Rhoa, Ruvbl1, Rac1, Ppp3ca, Ppp3cb were apparently upregulated in DT-PCA cells compared to SH-PAN cells, in accordance with our real-time PCR analyses (Fig. 2c).

In addition, we also validated the consistency between the real-time PCR results and microarray data in the other Wnt-associated 12 mRNAs (*Ppp3r1*, *Ppp2r1a*, *Skp1a*, *Ppp2r5e*, *Ctbp2*, *Wnt11*, *Wisp1*, *Mapk9*, *Ctbp1*, *Ppp2r5d*, *Plcb1* and *Cul1*) (Fig. S1).

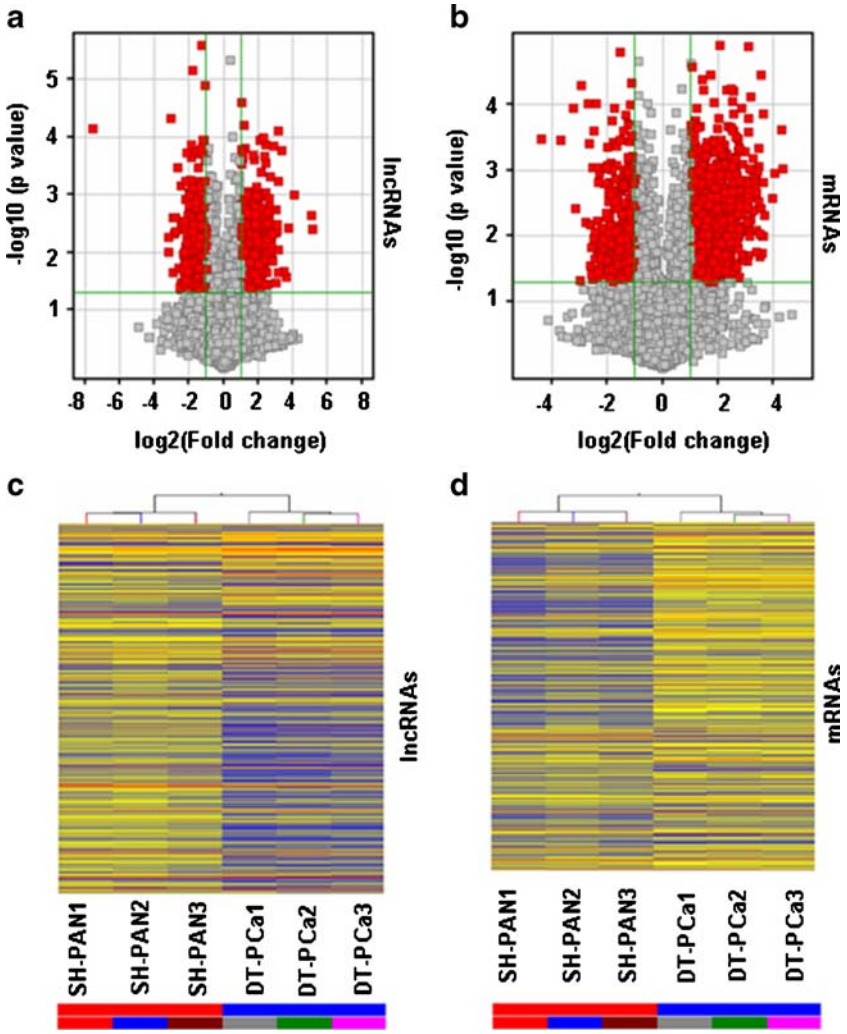

Fig. 1 The volcano plots and hierarchical clustering of microarray. (**a**, **b**) Volcano plots constructed using fold-change values and *p*-values are useful tools for visualizing differential expression between PanIN cell SH-PAN and PDAC cell DT-PCa. The *vertical lines* corresponded to 2.0-fold up and down and the *horizontal line* represented a *p*-value of 0.05. So the red point in the plot represented the differentially expressed lncRNAs or mRNAs with statistical significance ($n=3$). (**c**, **d**) Hierarchical clustering was performed based on differentially expressed lncRNAs or mRNAs between SH-PAN cells and DT-PCa cells. The dendrogram shows the relationships among the expression levels of the samples.

Table IV The Differentially Expressed Genes in Wnt Signaling Pathway

GeneSymbol	*p*-value	FCAbsolute	Regulation
Ppp3r1	0.006258534	8.37253	Up
Rac1	0.03764422	7.21344543	Up
Ppp3ca	0.028395372	6.362111	Up
Ppp2r1a	0.010671838	5.587456	Up
Rhoa	0.005992476	5.4853268	Up
Skp1a	0.034532134	5.1278867	Down
Ppp2r5e	0.002732564	4.4957304	Up
Ctbp2	0.027971473	4.350609	Up
Ruvbl1	0.01105962	4.2441235	Up
Ppp3cb	0.0326786	4.12865776	Up
Wnt11	0.021754133	2.8804677	Down
Wisp1	0.012546456	2.6125443	Up
Mapk9	0.015236075	2.4741156	Up
Ctbp1	0.002588035	2.3230038	Up
Ppp2r5d	0.000174728	2.253137	Up
Plcb1	0.008903006	2.1707544	Down
Cul1	0.006646779	2.1509397	Up

Tp53 Mutation Status Positively Correlates with High Expression of lincRNA1611 and *Ppp3ca* in PDAC

In order to identify whether $Tp53^{R172H}$ may directly promote the expression of the protein-coding genes, we conducted ChIP analysis in DT-PCa cells compared to SH-PAN cells. The results demonstrated that $Tp53^{R172H}$ directly acted on *Ppp3ca* and promoted the expression of *Ppp3ca* (Fig. 3a). However, the results concerning the other four genes, including *Ruvbl1*, *Rac1*, *Rhoa* and *Ppp3cb*, did not reveal direct interactions with $Tp53^{R172H}$ (data not shown). It indicates that $Tp53^{R172H}$ may increase the expression of *Ppp3ca*. Based on the fact that lincRNA1611 is the only one locates on the upstream of the nearby coding genes *Ppp3ca* (distance < 300 kb) among the 105 differentially expressed lincRNAs (≥2-fold changes), and the unknown expression and clinical significance of the *Ppp3ca* gene in PDAC, next, we compared the levels of *Ppp3ca* mRNA and HMlincRNA1611 (a human ortholog RNA of lincRNA1611) between 26 PDAC tissue samples and the matched normal pancreatic tissues by real-time PCR. Results showed that the expression of

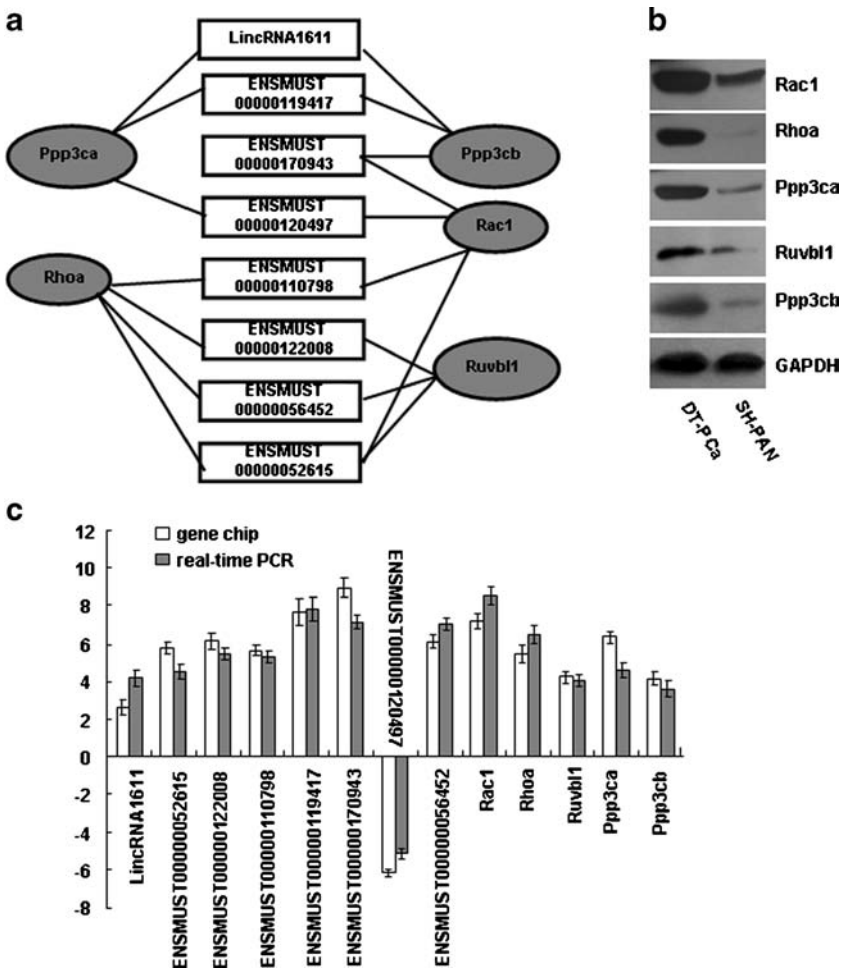

Fig. 2 Validation of the differentially expressed lncRNAs, mRNAs and proteins. (**a**) According to the coexpression network, five protein coding genes in Wnt pathway display a strong correlation with eight lncRNAs. (**b**) Comparison between microarray data and real-time PCR result. The *heights* of the columns in the chart represent the mean values of the fold changes in expression level and the *bars* represent standard errors of three independent experiments. The validation results of the 8 lncRNAs and 5 mRNAs showed that the microarray data correlated well with the real-time PCR results. (**c**) Western blot analysis confirmed that protein levels of Rhoa, Ruvbl1, Rac1, Ppp3ca, Ppp3cb in DT-PCa cells were apparently upregulated compared to SH-PAN cells.

HMLincRNA1611 ($p=0.001$) and *Ppp3ca* ($p=0.001$) was significantly higher in 22 PDAC tissue samples than that in matched normal pancreatic tissues (Fig. 3b), in which *Tp53* mutation were detected in 14 of 26 PDAC tissue samples.

Moreover, we detected the relationship between *Tp53* mutation status and lincRNA1611 levels or *Ppp3ca* mRNA levels (ΔCt value) in the fresh human pancreatic carcinoma specimens. Results showed that the expression of both lincRNA1611 and *Ppp3ca* in the 14 PDAC tissue with *Tp53* mutation were higher than that in the 12 PDAC tissue with wild type *Tp53*. *Tp53* mutation status displayed a strong positive correlation with lincRNA1611 levels($p=0.008$) or *Ppp3ca* mRNA level($p=0.015$) (Fig. 3c).

These results indicate that *Tp53* mutation may influence the expression of *Ppp3ca*.

Dynamic Alteration of *Ppp3ca* Expression in Human PDAC Tissues

Moreover, we detected the protein level of Ppp3ca in human PDAC tissue samples to evaluate the clinical significance in human pancreatic cancer. Immunohistochemistry was employed in 107 human PDAC tissues and paired peritumoral tissues. Of them, 29 PanIN-I tissues, 16 PanIN-II tissues and 27 PanIN-III tissues were observed by hematoxylin and Eosin (H&E) staining (Fig. 4a). Immunohistochemical results are summarized in bar chart and the percentage of cells with grade 0, 1, 2 and 3 staining (Fig. 4b). Ppp3ca expression was detected in 91 normal pancreatic tissues, 24 PanIN-I tissues and 13 PanIN-II tissues with low level staining (grades 0 and 1) of nucleus and cytoplasm. In contrast, Ppp3Ca expression was observed in 10 PanIN-III tissues and 62 PDAC tissues with high level staining (grades 2 and 3) of nucleus and cytoplasm.

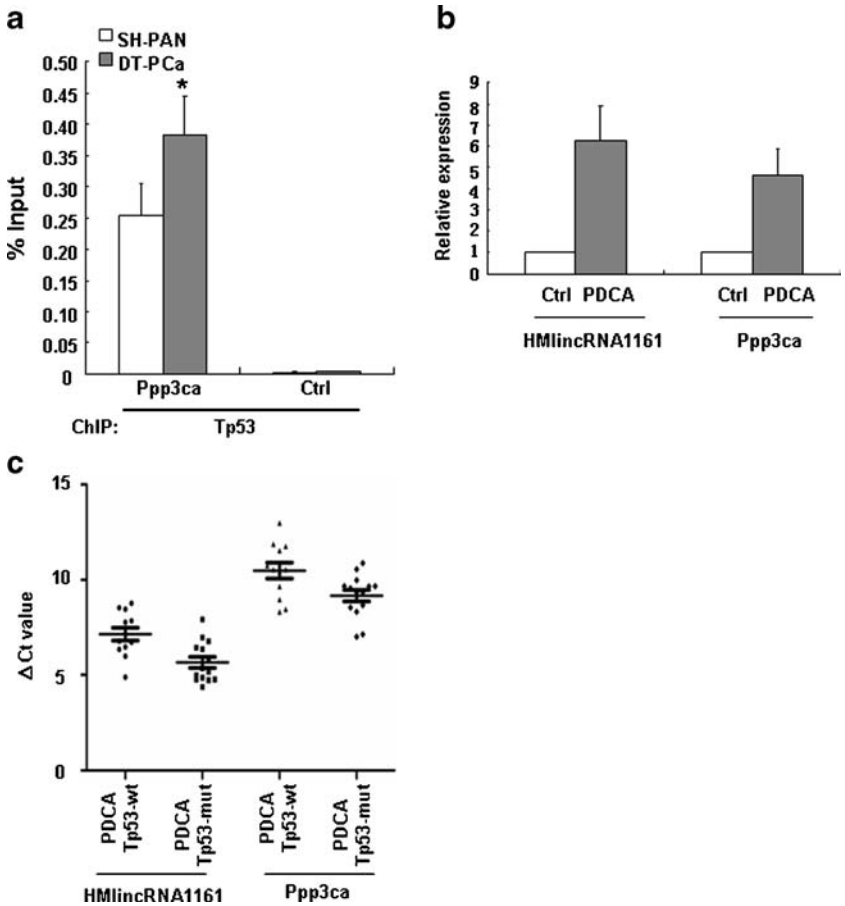

Fig. 3 The relationship between *Tp53* mutation and lincRNA1611 and *Ppp3ca* and the expression of lincRNA1611 and *Ppp3ca* in human PDAC tissues. (**a**). ChIP analysis of DT-PCa cells compared to SH-PAN cells were conducted by using the anti-tp53 antibody on *Ppp3ca* and GAPDH. Enrichment is determined relative to input controls. Results represented the mean values and the standard deviations of three independent biological replicates (*, $p<0.05$). (**b**) HMlincRNA1611 (human ortholog of lincRNA1611) and the protein-coding gene *Ppp3ca* in fresh human PDAC tissues and matched normal pancreatic tissues were validated by real-time PCR. The expression of HMlincRNA1611 and *Ppp3ca* was detected significantly higher in PDAC tissue samples than that in matched normal pancreatic tissues. (**c**) Real-time PCR was performed to compare the levels of lincRNA1611 and *Ppp3ca* in the PDAC tissue between with or without *Tp53* mutation. The expression of lincRNA1611 and *Ppp3ca* in PDAC tissue with *Tp53* mutation was significantly higher than that in PDAC tissue with wild-type *Tp53*.

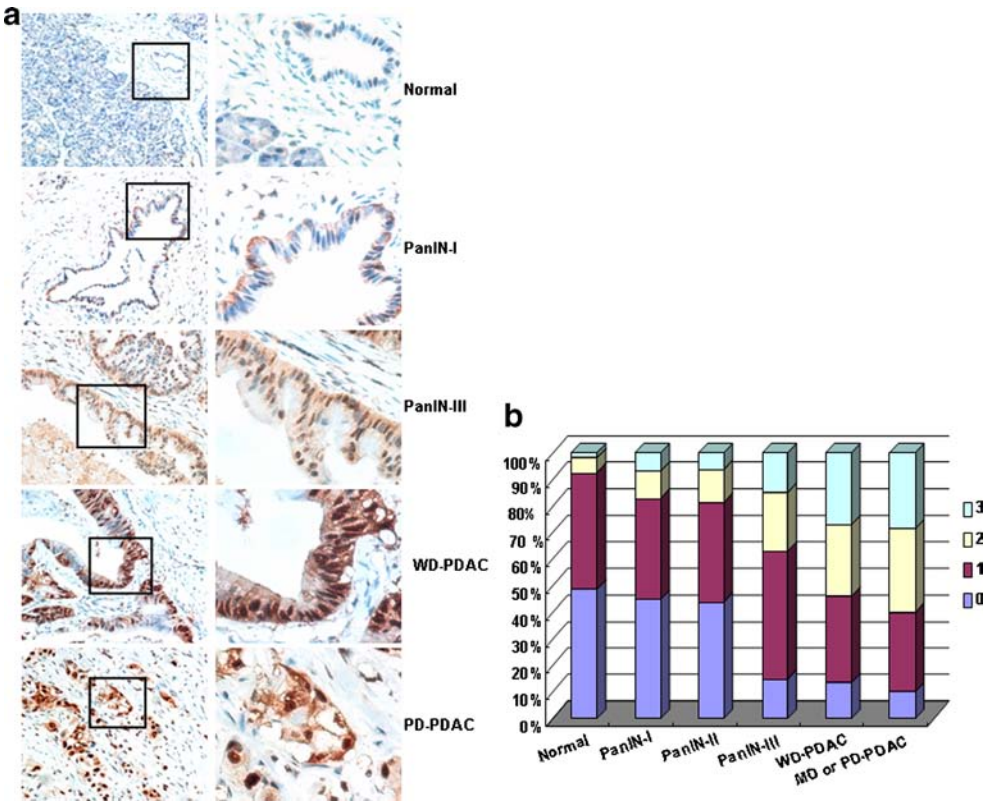

Fig. 4 *Ppp3ca* expression in human pancreatic neoplasias. (**a**) Immunohistochemical assessment of Ppp3ca levels was performed in paraffin-embedded human pancreatic carcinoma tissues, peritumoral PanIN-I tissues, PanIN-II tissues, PanIN-III tissues and peritumoral normal pancreatic tissues (*left panels*, ×200; *right panels*, ×400, are higher magnification of the boxes indicated in the *left panels*). The results are summarized in the *bar chart* (**b**), which shows the percentage of cells with grade 0, 1, 2 and 3 staining. Intense expression of Ppp3ca was observed in PDAC and PanIN-III tissues, while absent or weak expression was observed in normal pancreatic tissues, PanIN-I tissues and PanIN-II tissues.

These results indicate that the expression of lincRNA1611 and Ppp3ca is high in PDAC tissues, over-expression of lincRNA1611 and *Ppp3ca* is probably involved in PDAC.

DISCUSSION

Many researchers are drawing out an update view of lncRNA and proving the possible underlying molecular mechanism of some cancer-related lncRNAs. As known, a complicated progressive course through several signaling pathways and a series of gene mutations are involved in tumorigenesis. Of them, Wnt is one of the most cardinal signaling pathways and *Tp53* is one of frequent mutation genes in pancreatic carcinogenesis (21,22).

Our previous studies showed that expression of mutant *Kras* was sufficient to initiate PanINs, but it was not enough for developing invasive cancer (5,6,16). In *Pdx-1-Cre; LSL-Kras$^{G12D/+}$* mice of average age of 4.5 months, the majority of duct lesions in pancreas were low PanIN (PanIN IA and 1 B), rare PanIN III was observed, no carcinoma occurred. *Pdx-1-Cre; LSL-Kras$^{G12D/+}$*; *LSL-Tp53$^{R172H/+}$* compound mutant mice developed invasive pancreatic ductal adenocarcinoma. *Tp53^{R172H}* and *Kras^{G12D}* cooperate to promote widely metastatic pancreatic ductal adenocarcinoma in mice. Based on the detailed observation, PanIN cell line SH-PAN was isolated from the pancreas of a 4-month-old *Pdx-1-Cre; LSL-Kras$^{G12D/+}$* mutant mice, and a pancreatic ductal adeocarcinoma cell line DT-PCa was isolated from the pancreas of *Pdx-1-Cre; LSL-Kras$^{G12D/+}$*; *LSL-Tp53$^{R172H/+}$* compound mutant mice. Our study focused on displaying the lncRNAs expression profiles of genetically engineered mice cell lines, and the further explanation between the PanIN cells and PDAC cells. Differentially expressed lncRNAs/mRNAs between SH-PAN cells and DT-PCa cells were identified by microarray and the selected lncRNAs/mRNAs were tested and validated by real-time PCR. According to the microarray data and previous work, 8 lncRNAs and 5 mRNAs were selected to validate the consistency. LncRNA ENSMUST00000052615 is 914 bp intergenic RNA stems from the gene ENSMUSG00000045799 located on Chromosome 14. ENSMUST00000122008 is 522 bp intergenic RNA derived from the gene ENSMUSG00000060795 located on Chromosome 2. ENSMUST00000110798 is 1,360 bp intergenic RNA transcribed from the gene ENSMUSG00000079139 located on Chromosome 1. ENSMUST00000056452 is 971 bp intergenic RNA came from the gene ENSMUSG00000046341 located on Chromosome 4. LncRNAs ENSMUST00000052615, ENSMUST00000122008, ENSMUST00000110798 and ENSMUST00000056452 were predicted related to some protein-coding genes such as *Rhoa*, *Rwbl1* and *Rac1*. *Rhoa* gene encodes protein RhoA(Ras homolog gene family, member A). RhoA is part of a larger family of related proteins known as the Ras superfamily; proteins involved in the regulation and timing

of cell division. *Rac1* gene encodes protein Rac1. Rac1, also known as Ras-related C3 botulinum toxin substrate 1, is a protein found in human cells. Guo X *et al.* (23) showed that progression of pancreatic tumors is partially controlled by the balance between Tiam1-rac1 and RhoA. Timpson P *et al.* (24) indicated that *Tp53* mutation may drive pancreatic cancer cell invasion through spatial regulation of RhoA activity. Recent studies implicated the RuvbL1/RuvbL2 complexes in many cellular processes such as transcription, DNA damage response, snoRNP assembly, cellular transformation, and cancer metastasis (25). LincRNA1611 is 402 bp intergenic RNA from the gene CA585643 located on Chromosome 3. ENSMUST00000120497 is 207 bp antisense overlap RNA from the gene ENSMUSG00000084118 located on Chromosome X. ENSMUST00000170943 is 513 bp intergenic RNA from the gene ENSMUSG00000091223 located on Chromosome 3. ENSMUST00000119417 is 2,191 bp intergenic RNA from the gene ENSMUSG00000082896 located on Chromosome 3. ENSMUST00000170798 is 2,191 bp intergenic RNA from the gene ENSMUSG00000082896 located on Chromosome 3. The prognosis of several genes such as *Ppp3ca* and *Ppp3c* were associated with lncRNA ENSMUST00000120497, ENSMUST00000170943, ENSMUST00000170798 and LincRNA1611. *Ppp3ca* gene encodes protein Protein phosphatase 3, catalytic subunit, alpha isozyme(Ppp3ca) and *Ppp3cb* gene encodes protein Serine/threonine-protein phosphatase 2C catalytic subunit beta isoform(Ppp3cb). Recent studies showed that *Ppp3ca*, *Ppp3cb* were bound up with carcinogenesis (26–28).

Interestingly, we found that $Tp53^{R172H}$ could directly act on *Ppp3ca* in mouse cell lines and the expression of lincRNA1611 and *Ppp3ca* were high in human PDAC tissues. Furthermore, *Tp53* mutation status showed a strong positive relationship with the level of lincRNA1611 and *Ppp3ca* in PDAC. The expression of lincRNA1611 and *Ppp3ca* in PDAC tissue with *Tp53* mutation was significantly higher than that in PDAC tissue with wild-type *Tp53*. Therefore, we speculate that *Tp53* mutation induces the expression of *Ppp3ca*, the increased expression of HMlincRNA1611 and *Ppp3ca* may be associated with the progression of PDAC. However, how these lncRNAs act on and regulate the protein-coding genes still needs further study. Although we do not get sufficient evidence to utilize the 8 lncRNAs as the biomarkers in pancreatic carcinogenesis, the present data may help us to explore novel molecular markers in tumorigenesis.

The microarray also displayed a series of lincRNAs and the nearby associated protein-coding genes. In theory, overexpressing or silencing these lncRNAs may up-regulate or down-regulate the expression of their neighboring protein-coding genes. This is the first study that explores the expression profiling of lncRNAs in pancreatic cancer cells to elaborate pancreatic carcinogenesis. A collection of differentially expressed lncRNAs may play a part role as oncogenes or tumor suppressors in the progression of pancreatic carcinoma. Further work should be done to confirm whether these lncRNAs might regulate the known protein-coding oncogenes or tumor suppressors and determine whether they can serve as new therapeutic targets and diagnostic biomarkers in pancreatic carcinogenesis.

CONCLUSIONS

Our study provided an efficient and effective way to explore the alteration of lncRNAs or protein-coding genes associated with cardinal signaling pathways in the progression of carcinogenesis. The expression of lincRNA1611 and *Ppp3ca* was induced by *Tp53* mutation, which may be involved in progression of pancreatic cancer and serve as new therapeutic targets and diagnostic biomarkers for pancreatic cancer.

ACKNOWLEDGMENTS AND DISCLOSURES

We thank Professor David A Tuveson and Dr. Sunil R. Hingorani for genetically engineering mouse models of PanIN and PDAC, cell lines SH-PAN and DT-PCa, and helpful advices. Supported in part by National Natural Science Foundation of China (81272263, 30971130, 30672385), and Grant of Science and Technology Commission of Shanghai Municipality (11JC1407601).

REFERENCES

1. Siegel R, Naishadham D, Jemal A. Cancer statistics, 2013. CA Cancer J Clin. 2013;63:11–30.
2. Jemal A, Siegel R, Xu J, Ward E. Cancer statistics, 2010. CA Cancer J Clin. 2010;60:277–300.
3. Butturini G, Stocken DD, Wente MN, Jeekel H, Klinkenbijl JH, Bakkevold KE, *et al.* Influence of resection margins and treatment on survival in patients with pancreatic cancer: meta-analysis of randomized controlled trials. Arch Surg. 2008;143:75–83.
4. Vogelstein B, Kinzler KW. Cancer genes and the pathways they control. Nat Med. 2004;10:789–99.
5. Hingorani SR, Wang L, Multani AS, Combs C, Deramaudt TB, Hruban RH, *et al.* Trp53R172H and KrasG12D cooperate to promote chromosomal instability and widely metastatic pancreatic ductal adenocarcinoma in mice. Cancer Cell. 2005;7:469–83.
6. Shen R, Wang Q, Cheng S, Liu T, Jiang H, Zhu J, *et al.* The biological features of PanIN initiated from oncogenic Kras mutation in genetically engineered mouse models. Cancer Lett. 2013;339:135–43.
7. Yu M, Ting DT, Stott SL, Wittner BS, Ozsolak F, Paul S, *et al.* RNA sequencing of pancreatic circulating tumour cells implicates WNT signalling in metastasis. Nature. 2012;487:510–3.

8. White BD, Chien AJ, Dawson DW. Dysregulation of Wnt/beta-catenin signaling in gastrointestinal cancers. Gastroenterology. 2012;142:219–32.
9. Morris JP, Wang SC, Hebrok M, Hedgehog KRAS. Wnt and the twisted developmental biology of pancreatic ductal adenocarcinoma. Nat Rev Cancer. 2010;10:683–95.
10. Qiu MT, Hu JW, Yin R, Xu L. Long noncoding RNA: an emerging paradigm of cancer research. Tumour Biol. 2013;34:613–20.
11. Yu G, Yao W, Wang J, Ma X, Xiao W, Li H, *et al.* LncRNAs expression signatures of renal clear cell carcinoma revealed by microarray. PLoS One. 2012;7:e42377.
12. Han Y, Liu Y, Nie L, Gui Y, Cai Z. Inducing cell proliferation inhibition, apoptosis, and motility reduction by silencing long noncoding ribonucleic acid metastasis-associated lung adenocarcinoma transcript 1 in urothelial carcinoma of the bladder. Urology. 2013;8:209. e1-7.
13. Zhu Z, Gao X, He Y, Zhao H, Yu Q, Jiang D, *et al.* An insertion/deletion polymorphism within RERT-lncRNA modulates hepatocellular carcinoma risk. Cancer Res. 2012;72:6163–72.
14. Yuan SX, Yang F, Yang Y, Tao QF, Zhang J, Huang G, *et al.* Long noncoding RNA associated with microvascular invasion in hepatocellular carcinoma promotes angiogenesis and serves as a predictor for hepatocellular carcinoma patients' poor recurrence-free survival after hepatectomy. Hepatology. 2012;56:2231–41.
15. Yang F, Zhang L, Huo XS, Yuan JH, Xu D, Yuan SX, *et al.* Long noncoding RNA high expression in hepatocellular carcinoma facilitates tumor growth through enhancer of zeste homolog 2 in humans. Hepatology. 2011;54:1679–89.
16. Hingorani SR, Petricoin EF, Maitra A, Rajapakse V, King C, Jacobetz MA, *et al.* Preinvasive and invasive ductal pancreatic cancer and its early detection in the mouse. Cancer Cell. 2003;4:437–50.
17. Qian J, Niu J, Li M, Chiao PJ, Tsao MS. In vitro modeling of human pancreatic duct epithelial cell transformation defines gene expression changes induced by K-ras oncogenic activation in pancreatic carcinogenesis. Cancer Res. 2005;65:5045–53.
18. Wang Q, Liu H, Liu T, Shu S, Jiang H, Cheng S, *et al.* BRCA2 dysfunction promotes malignant transformation of pancreatic intraepithelial neoplasia. Anticancer Agents Med Chem. 2013;13:261–9.
19. Dong W, Shen R, Wang Q, Gao Y, Qi X, Jiang H. Y *et al.* Sp1 upregulates expression of TRF2 and TRF2 inhibition reduces tumorigenesis in human colorectal carcinoma cells. Cancer Biol Ther. 2009;8:2166–74.
20. Hotz B, Arndt M, Dullat S, Bhargava S, Buhr HJ, Hotz HG. Epithelial to mesenchymal transition: expression of the regulators snail, slug, and twist in pancreatic cancer. Clin Cancer Res. 2007;13:4769–76.
21. Froeling FE, Feig C, Chelala C, Dobson R, Mein CE, Tuveson DA, *et al.* Retinoic acid-induced pancreatic stellate cell quiescence reduces paracrine Wnt-beta-catenin signaling to slow tumor progression. Gastroenterology. 2011;14:1486–97.
22. Fiorini C, Menegazzi M, Padroni C, Dando I, Dalla Pozza E, Gregorelli A, *et al.* Autophagy induced by p53-reactivating molecules protects pancreatic cancer cells from apoptosis. Apoptosis. 2013;18:337–46.
23. Guo X, Wang M, Jiang J, Xie C, Peng F, Li X, *et al.* Balanced Tiam1-Rac1 and RhoA drives proliferation and invasion of pancreatic cancer cells. Mol Cancer Res. 2013;11:230–9.
24. Timpson P, McGhee EJ, Morton JP, von Kriegsheim A, Schwarz JP, Karim SA, *et al.* Spatial regulation of RhoA activity during pancreatic cancer cell invasion driven by mutant p53. Cancer Res. 2011;71:747–57.
25. Jha S, Dutta A. RVB1/RVB2: running rings around molecular biology. Mol Cell. 2009;34:521–33.
26. Gabrovska PN, Smith RA, Haupt LM, Griffiths LR. Investigation of two Wnt signalling pathway single nucleotide polymorphisms in a breast cancer-affected Australian population. Twin Res Hum Genet. 2011;14:562–7.
27. Singh AP, Bafna S, Chaudhary K, Venkatraman G, Smith L, Eudy JD, *et al.* Genome-wide expression profiling reveals transcriptomic variation and perturbed gene networks in androgen-dependent and androgen-independent prostate cancer cells. Cancer Lett. 2008;259:28–38.
28. Ostenfeld MS, Bramsen JB, Lamy P, Villadsen SB, Fristrup N, Sorensen KD, *et al.* miR-145 induces caspase-dependent and -independent cell death in urothelial cancer cell lines with targeting of an expression signature present in Ta bladder tumors. Oncogene. 2010;29:1073–84.